Optical Stark shift spectroscopy: Measurement of the $v=1$ polarizability in H_2

Mark J. Dyer and William K. Bischel*
Molecular Physics Laboratory, SRI International, Menlo Park, California 94025
(Received 12 November 1990)

We report a quantitative determination of the $v=1$ polarizability in H_2 by measuring the optical Stark shift and splitting of the $Q(0)$ and $Q(1)$ vibrational Raman transitions. For the $Q(1)$ transition, the $M_J=\pm1,0$ components are resolved, thereby allowing a determination of the polarizability anisotropy for the $v=1$ state. The measured optical Stark shift of the $Q(0)$ transition at 1060 nm is 23 MHz GW^{-1} cm^2, giving a polarizability difference between the $v=1$ and 0 states of $\Delta\alpha=0.49\pm0.03$ a.u., in good agreement with *ab initio* theory.

INTRODUCTION

The optical Stark effect will cause the rotational-vibrational energy levels in small molecules to shift and split due to the presence of a high-intensity nonresonant laser field. This effect has recently been observed for both vibrational [1] and rotational [2] Raman transitions in high-resolution Raman gain experiments using an optically applied Stark field. Because shifting of the energy levels effectively broadens the observed linewidths, it is one of the important mechanisms that limit the spectral resolution of coherent Raman experiments. Hence, the optical Stark effect has recently been included in the theory [3] of saturation processes in coherent anti-Stokes Raman spectroscopy (CARS). In other experiments, the broadening and shift of the anti-Stokes radiation generated by multiwave Raman mixing has been interpreted to be due to the optical Stark effect [4,5]. While all these experiments have tried to interpret their results based on order-of-magnitude estimates of the optical Stark effect, there have been no quantitative experiments that have used the nonresonant optical Stark effect to derive fundamental constants for the excited vibrational states of small molecules.

We report an experiment to use optical Stark spectroscopy for quantitative measurement of the polarizability and the polarizability anisotropy of the $v=1$ vibrational state in H_2. Hydrogen is a particularly interesting first molecule to study for a number of reasons. First, there are accurate *ab initio* calculations [6] of polarizabilities in H_2 that can be used to make a quantitative comparison between theory and experiment.

Second, accurate knowledge of the optical Stark shift in H_2 is of great practical importance in the design of Raman amplifiers and beam combining techniques [7] since H_2 is the gas most often used for stimulated Raman frequency conversion applications. For this application, it is quite important to know the polarizability of the $v=1$ in H_2 since the change in the polarizability between the $v=0$ and the $v=1$ vibrational states ($\Delta\alpha$) will determine the phase perturbations (and hence the beam quality) that occur across the spatial aperture of a large scale Raman amplifier [7]. The exact value of $\Delta\alpha$ has been an issue for a number of years due to the fact that there is a factor-of-2 discrepancy between current measurements [8] and *ab initio* theory [6]. An accurate measurement of the optical Stark effect for the vibrational Raman transition in H_2 would resolve this controversy.

The goal of our experiments was to measure the optical Stark effect for the $Q(0)$ and $Q(1)$ vibrational Raman transitions in H_2 and compare the measurements to *ab initio* theory. The energy levels and splittings in an optical field for the $Q(1)$ transition are illustrated in Fig. 1, where the magnitude of the shifts in units of MHz/(GW cm^{-2}) are calculated from the data presented in this paper and Ref. [6]. Without the high-intensity nonresonant optical field, the zero-pressure Raman frequency shift for the $Q(1)$ transition is 4155.247 ± 0.007 cm^{-1} as measured by Fourier-transform Raman spectroscopy [9]. When the nonresonant field is applied, there is a shift of the $v=0$ and 1 vibrational levels from their zero field values, and

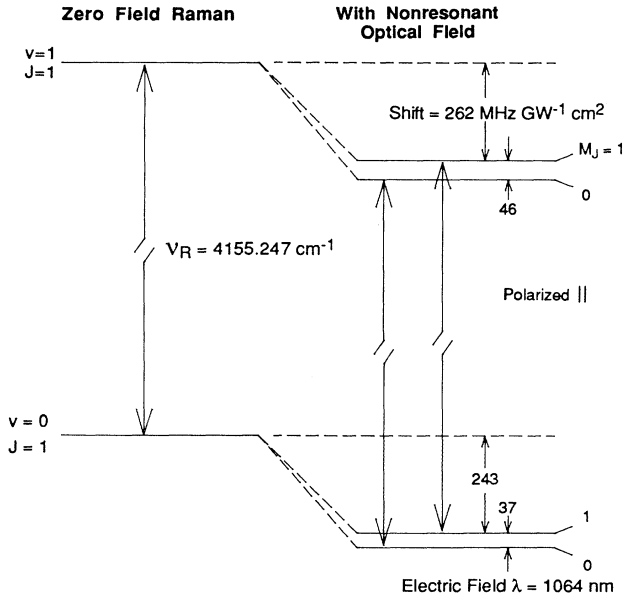

FIG. 1. Schematic illustrating level shifts of the $Q(1)$ branch in H_2 under the influence of a strong electric field.

the M_J degeneracy of the $J=1$ rotational level is split. (The $J=0$ levels will only show a shift since they are nondegenerate.) As illustrated in Fig. 1, the magnitude of shift in the vibrational levels (which is proportional to the average polarizability; see theory section) is approximately six times larger than the magnitude of the M_J splitting (which is proportional to the polarizability anisotropy). We can indirectly observe these energy-level shifts by carefully measuring the shift of the Raman transition frequency (illustrated by the arrows in Fig. 1) with and without the nonresonant field. The shift of the Raman frequency is due to the difference in the optical Stark shifts of the $v=0$ and 1 levels, and hence the Raman frequency would not change if the polarizabilities for these levels were the same (i.e., if $\Delta\alpha=0$).

In our experiments we use linear polarization for both the Raman pump-probe field and the nonresonant field. Therefore we have a selection rule of $\Delta M=0$ for the Raman transitions. As illustrated in Fig. 1, we expect to observe two Raman transitions for $M_J=0$ and ±1. The splitting between the $M_J=0$ and ±1 Raman transitions is only ~ 9 MHz/GW cm^{-2}) making these splittings extremely difficult to observe experimentally.

EXPERIMENT

The experimental apparatus is illustrated in Fig. 2 and consisted of a quasi-cw Raman gain spectrometer [10] using a Molectron MY-34 Nd:YAG (where YAG represents yttrium aluminum garnet) laser, modified and injection-locked to a Lightwave Electronics S-100 injection seeding system [11] as the pulsed pump laser source, and an argon-ion pumped Coherent CR699-29 Ring Dye Laser as the continuous tunable narrow-band probe laser. The Nd:YAG laser typically produces several hundred millijoules of transform-limited light at 1.06 μm in a 20-ns FWHM (full width at half maximum) duration, which when doubled to 532 nm yields a 14-ns pulse with a bandwidth of 22 MHz. The dye laser was operated at 683 nm to probe both the $Q(0)$ and $Q(1)$ transitions in H_2 with a few hundred milliwatts and a time-averaged bandwidth of roughly 8 MHz.

As shown in Fig. 2, both pump and probe beams were spatially filtered immediately after their sources, expanded and collimated with telescopes, then combined on a 683-nm dichroic mirror before being focused together by a 40-cm focal length lens into a cell containing hydrogen gas. The cell was constructed from stainless steel and designed for high pressure. Both ends of the cylindrical cell were sealed by fused silica windows with triple "V" antireflection coatings at the three wavelengths used here. The spot diameters at the input lens of the Raman cell were 1.6 and 2.1 cm for pump and probe, respectively, producing FWHM beam waists, which were scanned in profile by a 1-μm pinhole, of 25 μm in the center of the cell. Assuming a shift coefficient of 25 MHz GW^{-1} cm^2, this relatively tight focusing of the pump-probe beams meant that the energy of the 532-nm pump had to be held below 120 μJ for a 14-ns FWHM pulsewidth (an intensity of 1 GW/cm^2) in order to avoid more than a 5% shift or broadening contribution on a 500-MHz Raman linewidth by the 532-nm pump. Intensities at or below this level, however, provided adequate Raman gain signals at the hydrogen densities investigated, and the small Rayleigh ranges of the pump and probe allowed selection of a tight confocal parameter for the ir beam that would push the intensity of the applied optical field beyond 100 GW/cm^2, well above the intensity expected to resolve the shifted from unshifted line shapes.

The high-intensity nonresonant optical field was sup-

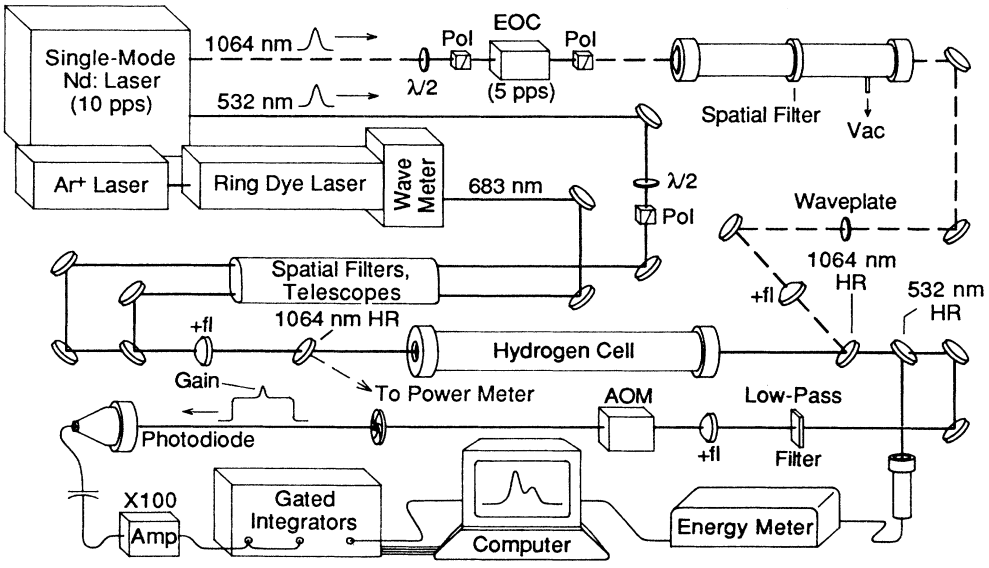

FIG. 2. Experimental layout for the measurement of the optical Stark effect in H_2.

plied by the residual ir fundamental of the Nd:YAG laser. The beam was first passed through a Laser Metrics Electro-Optic Chopper (EOC), then into a vacuum spatial filter, and collimated for delivery to the Raman cell. The chopper served dual purposes as a switch and a polarizer for the ir beam. The spatial filter under vacuum cleaned up the transverse mode quality of the beam and significantly reduced power fluctuations of the ir due to air particulates and pinhole breakdown. This ultimately proved vital in reducing broadening effects on the shifted line shape associated with ir field variations. The collimated ir beam was then passed through a 50-cm lens and counterpropagated against the pump-probe beams after being directed into the Raman cell by an ir high reflector (HR) transparent to the pump-probe combination. The waist of the beam, measured to be 75 μm in diameter at FWHM, was carefully positioned to overlap the waists of the pump and probe beams; the optical paths between laser source and cell center for the 1064- and 532-nm beams were made equal so that the peaks of both would overlap in time as well. Figure 3(a) shows the spatial profiles and Fig. 3(b) shows the temporal overlap achieved in the experiment. Upon exiting the cell, the ir beam was picked off by an identical ir dichroic reflector and sent into a power meter.

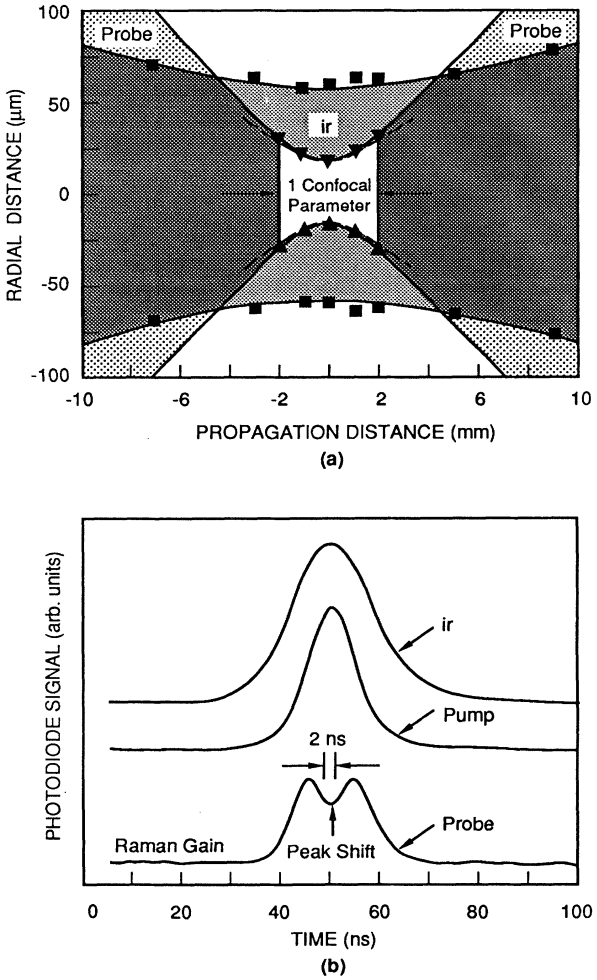

FIG. 3. Spatial and temporal overlap for optical Stark-shift measurements. (a) $1/e^2$ intensity data points for spatial cross sections of the ir and probe. The theoretical curves for the $1/e^2$ intensity plots for the ir probe and pump (dashed) beams are shown. Digitized oscilloscope traces (b) depict the time evolution of the ir, pump, and the Raman gain signal.

After passage through the Raman cell, the 532-nm pump was separated from the probe by a dichroic, measured and integrated by a pyroelectric energy detector and boxcar averager, and recorded by computer for normalization. The transmitted probe was down-collimated, filtered to remove residual pump light, mildly focused through an acousto-optic modulator (AOM) operating in first order, and sent into an EG&G FND 100 photodiode having a 1-ns rise-time response. The resulting gain signal detected by the photodiode exhibited the form of the 14-ns pump pulse shape superimposed atop the 200-μs-wide chopped CW probe background. This signal was enhanced through a 5–500-MHz bandpass, 20-dB gain Avantek amplifier, where the CW probe offset was filtered out, and sent into two SRS boxcar integrators operating with 2-ns gate widths and toggled at 5 Hz, half the trigger rate of the pump laser.

An example of the Raman gain signal is given in Fig. 3(b). The single-shot trace was acquired as the ring laser swept in frequency over the transition. The result of the optically induced Stark shift of the transition away from the probe frequency is manifested here as a dip in the gain signal at peak ir intensity. All boxcar channels were triggered off the Q-switched Nd:YAG laser oscillator cavity emission in order to reduce boxcar gate jitter on the signals to below 0.2 ns. The averaged output of the integrators were then recorded by computer. This entire arrangement made possible the controlled application of the ir field to the Raman interaction region on altering pulses of the pump laser as the frequency of the probe laser was tuned through the vibrational Raman transition, thus facilitating collection of shifted and unshifted spectral data on the same scan.

LINE-SHAPE ANALYSIS

Analysis of the data was performed on a DEC VAX 11/750 using a routine designed to remove the Gaussian laser linewidth contribution and then generate a fit to the experimental data. The line shapes used to fit the unshifted data were the theoretically predicted Lorentzian profiles, and the optical Stark-shifted data should, under conditions of a homogeneous, steady-state field, remain Lorentzian with a shift in frequency being the only distinction from the optical field-free data. The ir Stark field applied in our experiment, however, had Gaussian temporal and spatial mode distributions, so its slightly varied temporal and spatial behavior over the regions sampled in time and space contributed to a broadening of the ideal line shape. As a rule, our fits were started using the unshifted linewidth and allowing the peak position to be the

only adjustable parameter; then width and height parameters were freed to obtain the best fit to the side of the Lorentzian furthest from the unshifted line position. This method of analysis was based on the fact that the peak position is theoretically predicted to shift linearly with peak field intensity, and the part of the Lorentzian shifted the furtherst corresponds to gain in the region subjected to the most intense part of the ir field; hence, if there are intensity gradients away from the peak intruding upon the Raman gain region, the line shape will broaden in a direction favoring the lower intensities or smaller shifts. As an alternative, assuming nothing about the temporal and spatial distributions of the ir field, the data were also fit in entirety by floating all parameters, and although the differences in the fitting techniques were observable, shift results agreed to within the experimental error of the measurements.

RESULTS

Typical data are given in Fig. 4 at a density of 1.81 amagat of H_2 and a laser intensity of nearly 100 GW/cm^2. The observed shifts were density independent for both transitions in the absence of four-wave mixing for counterpropagating ir and pump-probe geometries. Polarizations of the pump and probe were identical for all measurements, and the ir polarization was initially fixed parallel to the pump-probe beams. Measurements involving different combinations of ir polarization and propagation direction were also made but the data will not be presented in this paper. Figures 4 and 5 show the raw data and fit as a function of frequency for an ir laser intensity of 100 GW/cm^2 and Fig. 6 graphs the dependence

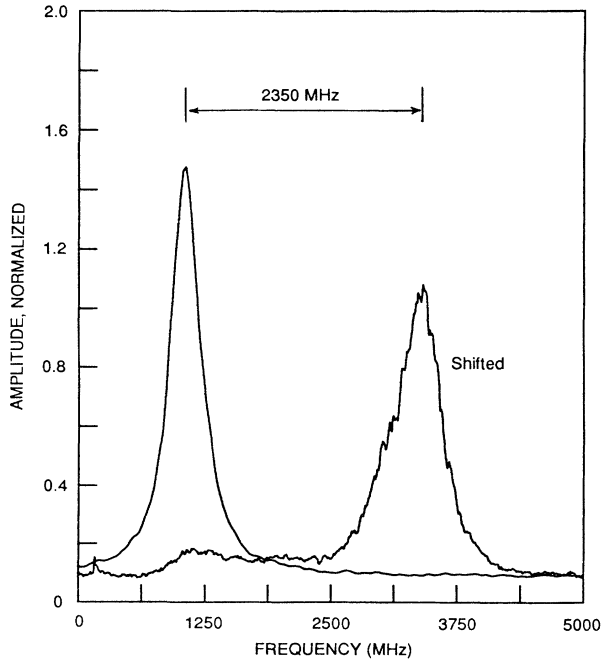

FIG. 4. Raman gain of the unshifted and shifted $Q(0)$ branch of H_2 at 1.81 amagat and 300 K.

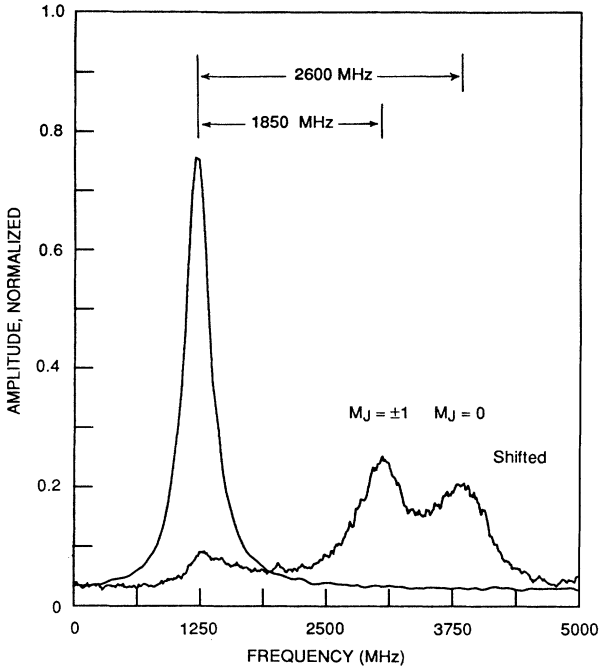

FIG. 5. Unshifted and shifted line shapes from Raman gain on the $Q(1)$ branch of H_2 at 1.81 amagat and 300 K.

of the optical Stark shift versus ir field intensity for the $Q(0)$ and $Q(0)$ transitions, along with a linear least-squares fit to each of the M_J levels undergoing the shift. For the $Q(0)$ transition (Fig. 6), the line shifts scaled with ir field intensity and the data yielded a shift coefficient of 23 MHz GW^{-1} cm^2. Shifting of the $Q(1)$ transition (Fig. 5) was measured to be 27 MHz GW^{-1} cm^2 for $M_J=0$ and 19 MHz GW^{-1} cm^2 for $M_J=\pm1$. The M_J splittings of a rovibrational level have been resolved, thus allowing the determination of the polarization anisotropy of the excited state.

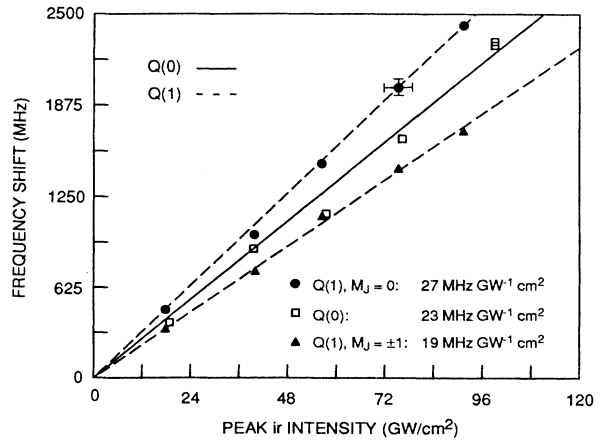

FIG. 6. Plot of the optical Stark shifts of $Q(0)$ and $Q(1)$ in H_2 vs peak ir intensity, and linear least-squares fits to individual M_J levels.

TABLE I. Wavelength dependence of the optical Stark shift for the $Q(0)$ and $Q(1)$ vibrational Raman transitions in H_2. 1 atomic unit (a.u.)$=1.481\,845\times10^{-25}$ cm^3.

Wavelength λ (nm)	Polarizabilities (a.u.)						Optical Stark shift $\Delta\nu_S$ (MHz GW^{-1}cm^2)		
	α_{00}	γ_{00}	α_{11}	γ_{11}	$\Delta\alpha$	$\Delta\gamma$	$Q(0)$	$Q(1)$ $M_J=0$	$Q(1)$ $M_J=\pm1$
∞	5.469	2.013	5.923	2.473	0.454	0.460	21	27	18
600	5.584	2.085	6.062	2.576	0.478	0.491	22	29	19
500	5.637	2.118	6.125	2.623	0.488	0.505	23	29	20
400	5.736	2.181	6.249	2.716	0.513	0.525	24	31	21
300	5.965	2.331	6.529	2.936	0.564	0.605	27	34	23
250	6.218	2.501	6.845	3.193	0.627	0.692	29	38	25
200	6.757	2.881	7.536	3.789	0.780	0.910	37	48	31

Uncertainties in the final fits were relatively small compared to the experimental uncertainty, which we conservatively estimate to be less than 10%, arising primarily from beam overlap and peak intensity measurement errors.

THEORY AND DISCUSSION

The optical Stark shift of a molecular rotational-vibrational level with quantum numbers v,J,M can be calculated from the following expression [2,12]:

$$\Delta E_{v,J,M}=-\tfrac{1}{4}[\alpha_v+C(J,M)\gamma_v](|E_0|^2)\ , \tag{1}$$

where α is the isotropic part of the polarizability $[\alpha_v=\frac{1}{3}(\alpha_\parallel+2\alpha_\perp)]$ and γ is the anisotropic part of the polarizability ($\gamma=\alpha_\parallel-\alpha_\perp$), E_0 is the ir laser field, and

$$C(J,M)=\frac{2}{3}\frac{J(J+1)-3M^2}{(2J+3)(2J-1)}\ . \tag{2}$$

Using the definition for the intensity $|E_0|^2=8\pi I/c$, where I is the peak ir laser intensity, we then calculate the optical Stark shift $\Delta\nu_S$ for a Q branch transition to be the difference in shifts between the upper and lower states,

$$\Delta\nu_S(\text{MHz})=46.8I\left[\frac{\text{GW}}{\text{cm}^2}\right][\Delta\alpha+C(J,M)\Delta\gamma]\ , \tag{3}$$

where we have introduced the notation $\Delta\alpha=\alpha_{11}-\alpha_{00}$ to denote the difference between the $v=1$ and the $v=0$ polarizabilities (similarly for $\Delta\gamma$). In Eq. (3), $\Delta\nu_s$ is in units of MHz, the polarizabilities are in atomic units (1 a.u.$=1.481\,845\times10^{-25}$ cm^3), and I is in units of GW/cm^2. The calculated optical Stark shifts as a function of wavelength are listed in Table I, where the wavelength-dependent polarizabilities are taken from Ref. [6]. We see from Table I that the optical Stark shift around $\lambda=1060$ nm ranges from 19 to 29 MHz GW^{-1}cm^2 for the different M_J components with an average value of 23 MHz.

The *ab initio* theoretical values from Table I are compared to the experimental measurements in Table II, where the agreement is surprisingly good for an experiment where the laser intensity had to be measured. Analysis of the $Q(1)$ shifts gives $\Delta\alpha=0.462\pm0.02$ and $\Delta\gamma=0.450\pm0.02$. No significant differences for $\Delta\alpha$ of $J=1$ and 0 were found. These results indicate that the $v=1$ excited-state polarizabilities can be accurately calculated for the simplest diatomic molecule (H_2), and provide a favorable basis to judge the accuracy of the calculations of the $v=1$ polarizability at other wavelengths as well as that of higher-order polarizabilities [6]. We can also compare our results to those of a previous experiment [13] that reported a shift of approximately -0.02 cm^{-1} for the $Q(1)$ transition under a field of about 30 GW/cm^2, which gives a shift coefficient of ~20 MHz GW^{-1}cm^2.

The difference in the index of refraction between $v=1$ and 0 (proportional only to $\Delta\alpha$) is also given in Table II to be 8.4%. This is compared with the only other experiments [8] that have measured this quantity to be 19%. We conclude that the previous experiments published a Δn that was too large by over a factor of 2. The practical

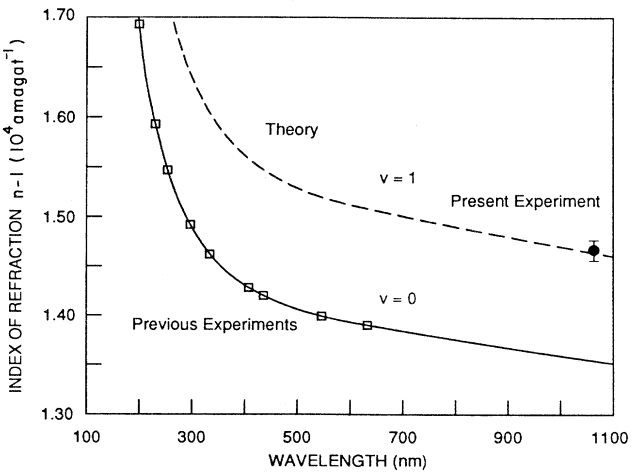

FIG. 7. Index of refraction of H_2 ($v=0$) and ($v=1$) vs wavelength. Experimental data for $v=0$ taken from Ref. [14].

TABLE II. Index of refraction measurement of H_2 ($v=1$) at $\lambda=1060$ nm using the Stark effect. Error bars are one standard deviation for the fit illustrated in Fig. 6.

	$\Delta\nu$ (MHz/GW cm^{-2})		$\Delta(n-1)_{av}$ (%)		
Transition	Expt.	Theory	Expt.	Theory	Ref. [8]
$Q(0)$	23.0±1.2	22			
$Q(1)$ $M_J=0$	27.0±0.7	28	8.4±0.3	8.4	19
$Q(1)$ $M_J=\pm1$	19.0±0.6	19			

consequence of this measurement is that the beam uniformity of the pump laser required for large scale Raman amplifiers [7] can be significantly relaxed from previously used values, thus reducing the overall cost of the device.

Finally, we illustrate in Fig. 7 the comparison between theory [6] and experiment for the absolute index of refraction for the $v=0$ state (where the data have been taken from Ref. [14]) and the $v=1$ state (data from the present experiment). Once again we see that the ground-state polarizabilities are well known and can be used to determine the absolute polarizability of the $v=1$ excited state.

CONCLUSION

We report a quantitative measurement of the average polarizability and the polarizability anisotropy of the $v=1$ excited state in H_2 from a measurement of the nonresonant optical Stark shift for the $Q(0)$ and $Q(1)$ Raman transitions. In these experiments the M_J splitting of the $Q(1)$ line has been observed, thus allowing the determination of the polarizability anisotropy. The results are in good agreement with *ab initio* theory, thus giving confidence in the ability of theory to predict higher-order polarizabilities in H_2.

ACKNOWLEDGMENT

We acknowledge support for this work from the Defense Advanced Research Projects Agency under Contract No. N000 14-8884-C-0256 through the Office of Naval Research.

*Present address: Coherent Inc., 3210 Porter Drive, Palo Alto, CA 94304.

[1] L. A. Rahn, R. L. Farrow, M. L. Koszykowski, and P. L. Mattern, Phys. Rev. Lett. **45**, 620 (1980).

[2] R. L. Farrow and L. A. Rahn, Phys. Rev. Lett. **48**, 395 (1982).

[3] M. Pealat, M. Lefebvre, J.-P. E. Taran, and P. L. Kelley, Phys. Rev. A **38**, 1948 (1988).

[4] William K. Bischel, Douglas J. Bamford, and Mark J. Dyer, Proc. SPIE **912**, 191 (1988).

[5] Wallace L. Glab and Jan P. Hessler, Appl. Opt. **27**, 5123 (1988).

[6] Winifred M. Huo, G. C. Herring, and William K. Bischel (unpublished).

[7] A. Flusberg and D. Korff, J. Opt. Soc. Am. B **3**, 1338 (1986).

[8] V.S. Butylkin, G. V. Venkin, L. L. Kulyuk, D. I. Maleev, V. P. Protasov, and Yu. G. Khronopulo, Pis'ma Zh. Eksp. Teor. Fiz. **7**, 474 (1974) [JETP Lett. **19**, 253 (1974)]; M. I. Baklushina, B. Ya. Zel'dovich, N. A. Mel'nikov, N. F. Pilipetskii, Yu. P. Raizer, A. N. Sudarkin, and V. V. Shkunov, Zh. Eksp. Teor. Fiz. **73**, 831 (1977) [Sov. Phys.—JETP **46**, 436 (1977)]; B. Wilhelmi and E. von Heumann, Zh. Prikl. Spectrosk. **19**, 550 (1973).

[9] D. A. Jennings, A. Weber, and J. W. Brault, Appl. Opt. **25**, 284 (1986).

[10] P. Esherick and A. Owyoung, *High Resolution Stimulated Raman Spectroscopy,* in *Advances in Infrared and Raman Spectroscopy,* edited by R. J. H. Clark and R. E. Hestor (Heydon and Son, Ltd., London, 1983).

[11] Mark J. Dyer, William K. Bischel, and David G. Scerbak, Proc. SPIE **912**, 32 (1988).

[12] W. H. Flygare, *Molecular Structure and Dynamics* (Prentice-Hall, Englewood Cliffs, NJ, 1978) p. 193.

[13] R. Farrow and L. Rahn, in *Raman Spectroscopy: Linear and Nonlinear* (Wiley, London, 1982), pp. 159 and 160.

[14] G.A. Victor and A. Dalgarno, J. Chem. Phys. **50**, 2535 (1969).